TOXICOLOGICAL SCIENCES **106(1)**, 193–205 (2008)
doi:10.1093/toxsci/kfn154
Advance Access publication July 26, 2008

PCB126 Exposure Disrupts ZebraFish Ventricular and Branchial but Not Early Neural Crest Development

Adrian C. Grimes,*,†,[1,2] Kyle N. Erwin,†,[2] Harriett A. Stadt,†,[2] Ginger L. Hunter,† Holly A. Gefroh,‡ Huai-Jen Tsai,§ and Margaret L. Kirby†,[3]

*Department of Molecular and Cellular Biology and Pathobiology, Medical University of South Carolina, Charleston, South Carolina 29425; †Duke University Medical Center, Department of Pediatrics, Neonatal-Perinatal Research Institute, Durham, North Carolina 27710; ‡Qualyst, Inc., Raleigh, North Carolina 27606; and §Institute of Molecular and Cellular Biology, National Taiwan University, Taipei, Taiwan 106

Received June 6, 2008; accepted July 14, 2008

We have used zebrafish and 3,3′,4,4′,5-pentachlorobiphenyl (PCB126) to investigate the developmental toxicity of polychlorinated biphenyls (PCBs) that exert their effects through the aryl hydrocarbon receptor (AHR). We found that cardiac and neural crest (NC)–derived jaw and branchial cartilages are specifically targeted early in development. The suite of malformations, which ultimately leads to circulatory failure, includes a severely dysmorphic heart with a reduced bulbus arteriosus and abnormal atrioventricular and outflow valve formation. Early NC migration and patterning of the jaw and branchial cartilages was normal. However, the jaw and branchial cartilages failed to grow to normal size. In the heart, the ventricular myocardium showed a reduction in cell number and size. The heart and jaw/branchial phenotype could be rescued by pifithrin-α, a blocker of p53. However, the function of pifithrin-α in this model may act as a competitive inhibitor of PCB at the AHR and is likely independent of p53. Morpholinos against p53 did not rescue the phenotype, nor were zebrafish with a mutant p53-null allele resistant to PCB126 toxicity. Morpholino knockdown of cardiac troponin T, which blocks the onset of cardiac function, prevented the PCB126-induced cardiac dysmorphogenesis but not the jaw/branchial phenotype. The cardiovascular characteristics appear to be similar to hypoplastic left heart syndrome (HLHS) and introduce the potential of zebrafish as a model to study this environmentally induced cardiovascular malformation. HLHS is a severe congenital cardiovascular malformation that has previously been linked to industrial releases of dioxins and PCBs.

Key Words: **zebrafish; ventricular development; valvulogenesis; cardiotoxicity; PCB126; aryl hydrocarbon receptor; proliferation; branchial cartilages.**

Heart development is impaired in many animal species by exposure to a number of environmental toxins including dioxins (Thackaberry *et al*., 2005) and polychlorinated biphenyls (PCBs) (DeWitt *et al*., 2006). Although industrial production of PCBs was stopped in the United States after 1978 due to concerns about accumulation, persistence, and toxicity, many are still released into the environment accidentally. PCBs are highly stable (congener-dependent half-life ranges from 1 day to 70 years) and lipophilic (WHO, 2000), resulting in biomagnification (Kuehl and Loffredo, 2006). Bioconcentration factors are very high for PCBs (Fox *et al*., 1994).

Many PCBs act through the aryl hydrocarbon receptor (AHR) pathway. This receptor is a member of the basic helix-loop-helix Per-Arnt-Sim family of transcriptional regulators. Although it has been studied intensively, its downstream targets and actual mechanisms of toxicity remain elusive (Schmidt and Bradfield, 1996). Both the AHR and its obligatory binding partner aryl hydrocarbon receptor nuclear translocation protein (ARNT) are found to be present at low levels in many embryonic tissues, with the highest levels in heart and neuroepithelium and neuroepithelial/NC-derived tissues such as visceral arches and otic and optic placodes (Abbott and Probst, 1995).

Several studies have been performed previously in which zebrafish and zebrafish embryos were exposed to PCBs and, specifically, 3,3′,4,4′,5-pentachlorobiphenyl (PCB126). Such PCBs accumulate in a dose-related manner and are effective inducers of hepatic ethoxyresorufin-O-deethylase activity, and have a negative effect on zebrafish reproduction (Orn *et al*., 1998). Zebrafish embryos exposed to Aroclor 1254, a mixture of PCB congeners that are common environmental contaminants, showed a reduction in expression of heat-shock protein 70 and serotonin in specific central nervous system neurons (Kreiling *et al*., 2007). In embryos, PCB126 induces cyp1a, cyp1b1, cyp1c1 and cyp1c2. While CYP1A may have a protective role against AHR agonists in liver and gut, CYP1B1, CYP1C1 and CYP1C2 may also play endogenous roles in eye and heart and possibly other organs, as well as during development (Jönsson *et al*., 2007a). A previous study has shown that PCB126 causes

[1] Present address: Departamento de Biología del Desarrollo Cardiovascular, Fundación Centro Nacional de Investigaciones Cardiovasculares Carlos III (CNIC), Melchor Fernández Almagro, 3 E-28029 Madrid, Spain.

[2] These authors contributed equally to the experimental work presented.

[3] To whom correspondence should be addressed at Duke University Medical Center, Department of Pediatrics (Neonatology), Box 3179, Room 157 Bell Research Building, Trent Drive, Durham, NC 27710. Fax: (919) 668-1599. E-mail: mlkirby@duke.edu.

a concentration-dependent *cyp1* gene induction in zebrafish embryos and that these embryos develop pericardial effusion by 3-days postfertilization (dpf) (Jönsson *et al*., 2007b). In addition, cell proliferation is depressed. Blocking AHR2 translation significantly inhibits these effects, showing that embryotoxicity is due to AHR2 activation (Jönsson *et al*., 2007b). However, morpholino knockdown of CYP1A in zebrafish embryos exposed to tetrachlorodibenzo-p-dioxin (TCDD), another strong AHR agonist, did not protect against the toxic effects of the TCDD, suggesting that the toxic effect of AHR agonists is independent of CYP1A (Carney *et al*., 2004). While other members of the CYP1 family could mediate the embryotoxicity, this has not been tested.

Evidence from several studies has suggested an association of hypoplastic left heart syndrome (HLHS) with environmental exposures to toxic compounds, and although additional genetic factors are implicated (Hinton *et al*., 2007), a definitive inherited pattern has yet to be established. Clusters of HLHS have been reported in at least two heavily industrialized regions of the United States: Maryland (Kuehl and Loffredo, 2006) and Wisconsin (Cronk *et al*., 2004). The epidemiological association of PCB with HLHS was recently published using data acquired during the Baltimore-Washington Infant Study (Ferencz *et al*., 1993). Kuehl and Loffredo (2006) show a link to the accidental release of PCBs and dioxins.

HLHS includes a suite of malformations characterized by abnormal development of the left heart and the aorta (Bharati and Lev, 1984). Severe forms of the syndrome can include aortic and mitral atresia along with almost nonexistent left ventricle, while milder manifestations may present with hypoplasia of the aortic and mitral valves and milder degrees of left ventricular hypoplasia. It is the most common cardiac cause of neonatal fatality, and its etiology is poorly understood.

In this study, we utilized zebrafish and PCB126, which is a model AHR agonist, to investigate the cardiotoxicity of such compounds and show that they affect the development of the atrioventricular and outflow valves, the smooth muscle component of the cardiac outflow tract, ventricular myocardium, and jaw and branchial cartilages. Ventricular cell cycle and growth are specifically arrested in the heart, and ventricular myocardial cell size is reduced. Because of the resemblance of the malformations and common causality of the defects, that is, PCB, and the genetic tractability of zebrafish, we propose that this is an excellent model system in which to investigate the etiology of environmental contaminant-induced HLHS.

MATERIALS AND METHODS

Fish Strains

Fish strains utilized included AB and Tübingen wild-type, Tg(*cmlc*::DsRed2-nuc) transgenics (Mably *et al*., 2003), a kind gift from Dr Kenneth Poss (Duke University) with permission from Dr C. Geoffrey Burns (Harvard Medical School), Tg(*cmlc2*::GFP) transgenics (Huang *et al*., 2003), a kind gift from Debbie Yelon (Skirball Institute, New York) with permission from Dr Huai-JenTsai (National Taiwan University, Taiwan), Tg(*Flk1*::EGFP)^{s843} transgenics (Jin *et al*., 2005), a kind gift from Dr Kenneth Poss (Duke University) with permission from Dr Suk-Won Jin (University of North Carolina, Chapel Hill), and the p53 mutant (ZIRC) (Berghmans *et al*., 2005). All experiments were performed using conditioned zebrafish system water (Nusslein-Volhard and Dahm, 2002).

PCB126 exposure. Healthy embryos at various stages of development from 5 to 48 h postfertilization (hpf) were selected for the experiments and transferred to 20-ml glass scintillation vials (12 embryos per vial, maximum). At approximately 5 hpf, water was removed from the vials and replaced with either 8 ml water containing various concentrations of PCB126 (AccuStandard, New Haven, CT, dissolved in dimethyl sulfoxide (DMSO) or water containing an equivalent volume of DMSO only (vehicle control). After 24 h, the exposure water was removed and replaced with clean fish water. Embryos were then incubated at 28.5°C and observed periodically for the development of phenotype. Experiments were performed in triplicate. The optimum dose of PCB126 to produce a uniform, fully penetrant phenotype in greater than 90% of the embryos using this protocol was found to be 7.5 μg/l. The protocol was tested independently on several hundred embryos by several different investigators.

Pifithrin-α treatment. Following similar protocols to those described above, embryos were exposed to either 7.5 μg/l PCB126 or DMSO (vehicle control) or 7.5 μg/l PCB126 supplemented with doses of 1μM pifithrin-α. Pifithrin-α was tested at doses to ascertain the optimal rescue conditions. In these experiments, concentrations of 0.1, 0.5, 1.0, 5, and 10μM were used. In all, 1.0μM pifithrin-α gave the most consistent rescue. Additionally, pifithrin-α was found to be lethal at doses much higher than 1μM, and so the 1μM dose was chosen for all the co-incubation experiments with PCB126. Because pifithrin-α is also maintained in a DMSO stock solution, the DMSO concentration in controls was adjusted accordingly. After 24 h, exposure water was removed and replaced with either fresh pifithrin-α solution or fresh water containing an appropriate concentration of DMSO. Embryos were then incubated at 28.5°C and observed periodically for the development of phenotype. Because pifithrin-α is light sensitive, for these experiments, embryos were maintained at 28.5°C in the dark.

Cardiomyocyte counting. Using a transgenic fish that expresses *Discosoma* red fluorescent protein in cardiomyocyte nuclei (Tg[*cmlc2*::DsRed2-nuc]), the PCB126 exposure regime described above was followed. Fish from control and PCB126-exposed groups at 48 and 72 hpf were anesthetized, and their hearts were excised. The hearts were mounted in 3% methylcellulose in fish water on glass microscope slides and coverslipped before being imaged by deconvolution microscopy using a Leica DM RAZ microscope equipped with a fluorescence imaging system. Cells of the atrium and ventricle were differentiated by a constriction at the atrioventricular border and by the fact that atrial nuclei are more round and less closely associated than those of the ventricle. Cells from six hearts for each group were counted, and the data were analyzed using student's *t*-test.

Immunohistochemistry. Immunohistochemistry was performed essentially as previously described (Grimes *et al*., 2006), with the following exceptions. For experiments to determine cardiomyocyte size, PCB-exposed and control Tg(*cmlc*::DsRed2-nuc) fish of various stages were anesthetized in 0.016% tricaine containing 0.1M potassium chloride to relax the heart chambers in diastole. Fish were fixed for 1 h at room temperature in 2% paraformaldehyde in phosphate-buffered saline (PBS) (pH 7.4) supplemented with 5% sucrose, dehydrated in methanol series, and stored at − 20°C for 24 h. After rehydration into PBST (PBS, 0.1% Tween 20), fish were treated with 2 μg/ml proteinase K dissolved in water for 5, 15, or 25 min (for 48, 72, and 96 hpf, respectively). After rinsing twice in PBST, fish were washed in PBST containing 0.1% DMSO for 15 min, blocked in antibody solution (PBS with 10% [vol/vol] sheep serum; 2 mg/ml bovine serum albumin; 0.2% [wt/vol] saponin; 0.1% [vol/vol] DMSO) for 1 h, and then incubated with 1:1000 Living Colors anti-DsRed polyclonal antibody (Clontech Laboratories, Moutain View, CA) and 1:500 Zn5 monoclonal antibody (ZFIN, Eugene, OR) overnight at 4°C

in antibody solution as above. After rinsing four times for 15 min each in PBST/0.1% DMSO, embryos were incubated for 2 h at room temperature in the dark with 1:200 AlexaFluor 568 goat anti-rabbit IgG(H+L) and 1:200 AlexaFluor 488 goat anti-mouse IgG(H+L) secondary antibodies (Molecular Probes, Eugene, OR) in antibody solution as before. This protocol allowed visualization of cardiomyocyte borders in green and nuclei in red.

For experiments to determine endocardial development, PCB-exposed and control Tg(*Flk1*::EGFP)^{s843} fish of various stages were anesthetized in 0.016% tricaine containing 0.1M potassium chloride as above. Fish were fixed for 1 h at room temperature in 2% paraformaldehyde in PBS (pH 7.4), and the remainder of the protocol was performed essentially as described above but without DMSO supplementation of the buffers. In this case, primary antibodies used were 1:1000 anti-GFP polyclonal (Millipore, Temecula, CA) and 1:20 anti-myosin monoclonal MF20 (Developmental Studies Hybridoma Bank, University of Iowa, IA). Secondary antibodies were 1:200 AlexaFluor 568 goat anti-mouse IgG_{2b} and 1:200 AlexaFluor 488 goat anti-rabbit IgG(H+L). This protocol allowed visualization of myocardium in red and endocardium in green. Following labeling, hearts were excised and either imaged using epifluorescence microscopy or by confocal as described above. A total of 24 PCB-exposed and 24 control fish were analyzed for each stage (48, 72 and 96 hpf). Six PCB-exposed and six control fish (three for each treatment at both 48 and 96 hpf) were imaged by confocal.

Alcian blue cartilage staining. In all, 96 hpf embryos from control, PCB126-exposed, and PCB126/pifithrin-α cotreated groups were anesthetized in 0.016% tricaine, fixed in 3.7% neutral buffered formalin (pH 7.0) at room temperature overnight, and then transferred to a 0.1% solution of Alcian blue dissolved in 80% ethanol/20% glacial acetic acid. After staining overnight, embryos were rinsed in ethanol, rehydrated in an ethanol series, and had the pigment bleached with 3% hydrogen peroxide/1% potassium hydroxide for 30 min. Tissues were cleared in 0.05% trypsin dissolved in a saturated solution of sodium tetraborate for 3 h. Stained embryos were mounted in 80% glycerol prior to imaging.

Visualization of outflow tract development. To monitor development of the smooth muscle component of the cardiac outflow tract (the bulbus arteriosus), live control and PCB-exposed Tg(*cmlc2*::GFP) zebrafish at various stages were transferred from fish water directly into a 10μM solution of DAR-4M (Calbiochem, San Diego, CA) in fish water adjusted to pH 7.0, and incubated overnight in the dark. Following incubation, embryos were either visualized *in vivo* or fixed in preparation for further immunohistochemical labeling as above. DAR-4M is a red fluorescent nitric oxide indicator that labels the bulbus arteriosus from early developmental stages similarly to the fluorescein-based DAF-2DA as has been previously described (Grimes *et al.*, 2006).

Paraffin embedding and sectioning. Following whole-mount visualization of DAR-4M and MF20 immunohistochemical labeling, selected embryos dehydrated in methanol series and cleared in 2:1 benzyl benzoate:benzyl alcohol. After clearing, embryos were transferred directly to xylenes and allowed to equilibrate for 5 min prior to being placed in paraffin and maintained at 60°C for 90 min. Embryos were embedded in disposable plastic moulds and allowed to cool before being sectioned at 8 μm on a Leica RM2155 microtome, mounted on glass sides, and dried overnight in the dark. The following day, slides were heated to 60°C, placed in xylenes for 5 min, rehydrated through an ethanol series to water, and coverslipped using warmed ProLong Gold Antifade Reagent with 4′,6-diamidino-2-phenylindole (DAPI).

TUNEL labeling. Vehicle control and PCB126-exposed embryos were collected at 24, 36, 48, 60, and 72 hpf. As a positive control, prior to each time point, a third group was incubated for 6 h in fish water containing 500nM camptothecin, a topoisomerase I inhibitor that induces apoptosis. Fish were anesthetized in 0.016% tricaine and fixed in 4% paraformaldehyde in PBS (pH 7.4) overnight at 4°C and prepared for paraffin embedding and sectioning as above. After paraffin removal in xylenes and rehydration, sections were digested in 10 μg/ml proteinase K for 5 min, rinsed once in distilled water, and twice in PBS (pH 7.4). Cell death was visualized using the ApopTag Red Kit (Chemicon, Temecula, CA) following manufacturer's instructions. Sections were colabeled with anti-myosin MF20 and coverslipped using DAPI as previously described.

BrdU incorporation. Vehicle control and PCB126-exposed embryos were collected at 24, 36, 48, 60 and 72 hpf and placed in a solution of fish water containing 10mM BrdU/15% DMSO in tissue culture dishes over a 4°C ice-water bath for 30 min. Embryos were rinsed three times with fish water, incubated for 30 min at 28.5°C, anesthetized in 0.016% tricaine, and fixed in methacarn for 1 h at room temperature. Following dehydration in ethanol, embryos were processed for paraffin embedding and sectioning as previously described. After paraffin removal in xylenes and rehydration, sections were treated with 5% hydrogen peroxide in methanol, rinsed in water, and then digested with 10 μg/ml proteinase K for 5 min. Following a further rinse in water, sections were treated with 2N HCl for 45 min at 37°C, washed twice in borate buffer (70mM boric acid/9mM sodium borate), twice in 0.1M Tris buffer (pH 7.0), and then blocked for 1 h in Tris/2% fetal bovine serum (FBS). Sections were incubated for 1 h with anti-BrdU antibody (Roche, Nutley, NJ) in Tris/2% FBS, rinsed in Tris, and reblocked before incubating with AlexaFluor 488 secondary antibody (1:200 in Tris/2% FBS). Sections were colabeled with anti-myosin MF20 and coverslipped using DAPI as previously described.

Confocal imaging to determine cell size and disruption of endocardium. To determine cell size, the hearts from control and PCB-exposed Tg(*cmlc2*::DsRed2-nuc) zebrafish were labeled in whole mount using anti-DsRed and Zn5 antibodies as described above, the hearts excised, and imaged using a Zeiss LSM510 on an Axiovert200 motorized inverted stand. Still, composite images were compiled and mean cell size calculated using using CellProfiler software (Carpenter *et al.*, 2006), according to the instructions provided. Similarly, to determine disruption to endocardium, Tg(*Flk1*::GFP) fish were labeled in whole mount using anti-GFP and MF20 antibodies. Embryos at 48 hpf were imaged as above in whole mount. At 96 hpf, the hearts were excised and imaged as above.

Primers and PCR Conditions

AP2a Forward: 3′-GACTGAGTTTCCAGCCAAGG-5′;
AP2a Reverse: 3′-GCTTTAATTGCCTCCGTCAG-5′;
AP2b Forward: 3′-GCGACACTGAAGCAAGTGAA-5′;
AP2b Reverse: 3′-AGCTATTGCCAGCACAGGTT-5′;
CYP1A (accession ID: AF210727)
Forward: 5′-CGACTGCAAAGAGAATTGGA-3′;
Reverse: 5′-CTTTGGATGTGCAGTGAGGA-3′;
β-actin (accession ID: AF057040)
Forward: 5′-AAGATCAAGATCATTGCTCC-3′;
Reverse: 5′-CTGTTTAGAAGCACTTCCTG-3′;
prtfdc1 hypoxanthine-phosphoribosyl transferase (*HPRT*) (accession ID: AY181981)
Forward: 5′-GTTCATAAGAAATGCCATTGTGGA-3′;
Reverse: 5′-TCAAATCCCACATAGTCTGGC-3′.

For RNA extraction, embryos were homogenized, and total RNA was isolated using TRIZOL reagent (Invitrogen, Carlsbad, CA), digested with RQ1 DNase (Promega, Madison, WI), and further purified using an RNeasy Mini Kit (Qiagen, Valencia, CA). RNA concentration was determined using a NanoDrop ND-1000 spectrophotometer (NanoDrop, Wilmington, DE), and quality was verified using an Agilent 2100 bioanalyzer. First-strand cDNA was generated from 2 μg total RNA with SuperscriptII Reverse Transcriptase (Invitrogen) and oligo dT primers in 20-μl reactions. cyp1a, β-actin, and hprt cDNAs were PCR amplified separately in triplicate using a Bio-Rad iCycler iQ. In all, 2 μl cDNA was PCR amplified in a 25-μl reaction volume using iQ SYBR Green Supermix (Bio-Rad, Hercules, CA). Real-time PCR reaction conditions were 95°C for 5 min followed by 40 cycles of 94°C for 20 s, 57°C for 20 s, and 72°C for 30 s with a final extension of 7 min at 72°C. Formation of specific products was verified through melting curve analysis and electrophoresis. *cyp1a* expression was quantified relative to DMSO control and normalized against β-actin and

hprt using REST 2005 (Relative Expression Software Tool) using PCR efficiency in the calculation.

Morpholinos

The p53 morpholino (5′-GCGCCATTGCTTTGCAAGAATTG-3′) targets the start site and was originally used and characterized by Langheinrich *et al.* (2002) and recently reported by Robu *et al.* (2007) to block apoptosis.

The tnnt2 morpholino (5′-CATGTTTGCTCTGATCTGACACGCA-3′) (Sehnert *et al.*, 2002) targets the start site.

GeneTools standard control morpholino (CCTCTTACCTCAGTTACAATTTATA) was used as negative control.

We injected 4-15 ng of the morpholino oligo into embryos at the 1−4 cell stage.

RESULTS

The PCB126-Induced Heart Phenotype

A screen of various environmental contaminants showed that PCB126 induced consistent dysmorphogenesis of the heart, jaw, and branchial cartilages (Fig. 1) across a range of concentrations from 1 to 50 μg/l, with mortality increasing at higher concentrations. Exposures at 7.5 μg/l initiated from 5 to 24 hpf produced a consistent and penetrant phenotype in greater than 90% of embryos, with minimal mortality before 96 hpf, although the embryos rarely survived beyond 120 hpf. Exposure could be administered up to 36 hpf for a period of 24 h with similar results. Initiation of the treatment after 36 hpf no longer produced the same phenotype. While the trunk and tail developed normally, at 96 hpf, the heart could clearly be seen stretched across the distended pericardial sac (Fig. 1C). Alcian blue staining demonstrated that, while there was a severe reduction in size of the jaw and branchial cartilages, the patterning itself did not appear to be affected (Figs. 1D–G).

Using Tg(*cmlc2*::GFP) transgenic fish, the bilateral heart fields were visible by 20 somites, and heart field migration, fusion to form the initial heart tube, and the overall size and morphology of the heart up to approximately 24 hpf were similar in exposed and vehicle control fish. Chamber specification also appeared normal, based on the presence of a constriction at the atrioventricular border and the expression of cardiac-specific markers (Figs. 1H–K). In addition, there was little sign of pericardial effusion until after 24 hpf in most fish exposed to the compound (Figs. 2A and 2B). Heartbeat and contractility appeared normal. However, by 36 hpf, pericardial effusion and blood pooling at the cardiac inflow appeared in the PCB126-exposed embryos (Figs. 2C and 2D). Signs of heart failure increased over the next 60 h of development, with ventricular contractions and circulation abolished by 96 hpf. Atrial contractions persisted until after 96 hpf.

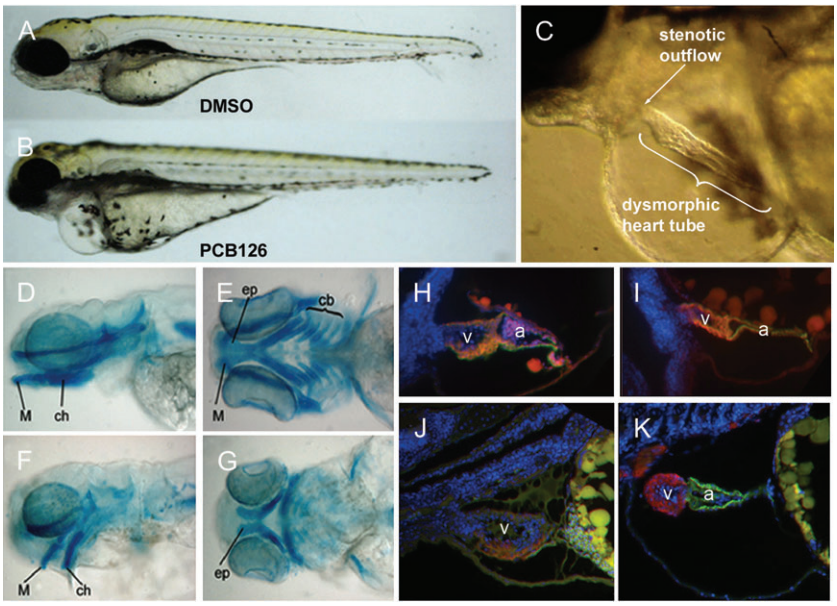

FIG. 1. Jaw and heart phenotype after PCB126 exposure. (A–G) and (J–K) are 96 hpf embryos. (A) Vehicle control (DMSO). (B) PCB126-exposed embryo, showing truncation of the jaw and obvious pericardial effusion. (C) Detail of the heart, lateral view, cranial to the left, showing the absence of a bulbus arteriosus, a stenotic outflow, and a dysmorphic heart tube. (D–G) Alcian blue staining of the jaw and branchial cartilages. Lateral (D, F) and ventral (E, G) views. (D, E) Vehicle control (DMSO). (F, G) PCB126 exposed. The jaw and branchial cartilages in the PCB126-exposed embryos are present and patterned correctly but are diminished in size and underdeveloped. Note the incomplete fusion of the ethmoid plate (ep) and the almost dorsoventral orientation of the ceratohyal (ch) and Meckel's cartilage (M); cb, ceratobranchials. (H–K) are histological sagittal sections through the heart immunolabeled with S46 (atrium, green or yellow) and MF20 (ventricle, red). (H, I) are 46 hpf and (J, K) are 96 hpf. Both the DMSO-treated controls (H, J) and the PCB126-treated embryos (I, K) show atrial (a) and ventricular (v) chamber specification. The atrium cannot be seen in the normal embryo at 96 hpf shown in (J) because it is out of the plane of section as the heart has looped properly. The atrium can be seen in the PCB-treated embryo (K) because the heart has not looped. The AVC has formed as indicated by the constriction between the atrial and ventricular chambers.

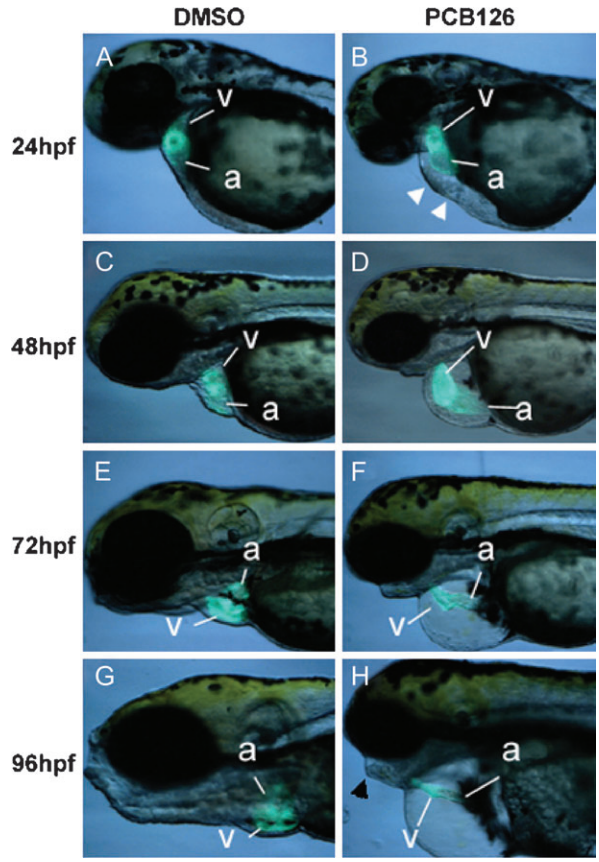

FIG. 2. Progression of the heart phenotype. Two individual Tg(*cmlc2*::GFP) fish, imaged sequentially at 24, 48, 72, and 96 hpf. Lateral views, cranial to the left. (A), (C), (E), and (G) are of a control fish (DMSO); (B), (D), (F), and (H) are of a PCB126-exposed fish. (A, B) At 24 hpf, there is little discernable morphological difference between the hearts of these fish, although some mild pericardial effusion can be observed in a few exposed (white arrowheads in B). (C, D) By 48 hpf, the heart of the control fish (C) has undergone looping, the atrium now lying to the left of the ventricle. In the exposed fish (D), pericardial effusion is pronounced and the heart obviously dysmorphic. (E, F) By 72 hpf, the atrium of the control fish (E) has rotated to adopt its position almost dorsal to the ventricle. The heart of the exposed fish (F) is considerably smaller and appears stretched across the effused pericardial cavity; the atrium lies caudal to the ventricle. Note that even compared to its own size at 48 hpf, the heart of the exposed fish is dramatically reduced in size. (G, H) By 96 hpf, the exposed fish (H) has extreme pericardial effusion, and the heart appears further diminished in size. Note also the truncated jaw (black arrowhead in H). a, atrium; v, ventricle.

The heart failed to loop correctly and by 48 hpf appeared to be stretched across the enlarging pericardial cavity. By 72 hpf, the heart was a linear tube, had diminished in size, and beat erratically. By 96 hpf, pericardial and yolk sac effusion were extreme, and the heart had become a narrow tube with severely reduced diameter. The heart size was reduced not only in comparison to vehicle controls but also to its own size earlier in development (compare Figs. 2C and 2H).

Using DAR-4M, which, similarly to DAF-2DA, labels the bulbus arteriosus from its earliest development (Grimes *et al.*, 2006), we showed that the bulbus failed to develop properly and by 96 hpf was diminished in length and diameter compared to controls. Normally, the bulbus is added to the heart between 48 and 96 hpf and, through development, its attachment to the ventricular outflow moves from a cranial branchial position to a more caudal position within the pericardial cavity. In PCB126-exposed embryos, the outflow remained attached to the cranial limit of the pericardial cavity, just under the jaw.

Because pericardial effusion could contribute to the heart phenotype, we provided osmotic support to PCB126-exposed embryos using 175mM mannitol (Hill *et al.*, 2004). While this prevented the development of both pericardial and yolk sac effusion, it had little impact on the development of cardiac and branchial cartilage phenotypes. By 96 hpf, the bulbus was reduced, and the heart had failed to loop, remaining considerably smaller than in controls (data not shown).

NC Migration, Patterning, and Differentiation Are Unaffected

Because the AHR is highly expressed in NC-derived tissues (Abbott and Probst, 1995) and evidence exists that NC cells contribute to zebrafish myocardium in addition to the jaw and branchial cartilages (Li *et al.*, 2003; Sato and Yost, 2003), we analyzed NC development using *crestin* (Luo *et al.*, 2001) or *AP2-α* (Li *et al.*, 2003). We saw no difference in either the level or pattern of message expression between control and PCB-exposed fish (Supplementary Fig. 1). These data suggest that, while NC-derived tissues are affected by PCB126, the phenotype does not arise from an impairment of NC migration, patterning, or differentiation. NC cells adopt their correct positions but subsequently fail to grow correctly, even though they appear to differentiate as cartilage at the appropriate time.

PCB126 Does Not Cause Increased Cell Death but Blocks Ventricular Proliferation

While cell death could cause PCB126-exposed hearts to diminish in size over time, TUNEL assays showed that the phenotype was not caused by increased cell death (Supplementary Fig. 2). There was an almost complete lack of TUNEL labeling in the branchial cartilages or myocardium of control and PCB126-exposed embryos at all time points examined. Results were confirmed with two additional markers of cell death, acridine orange and anti-caspase 3 (data not shown). The effectiveness of the protocols was confirmed using a positive control, camptothecin, which induced high levels of cell death in all tissues (Supplementary Fig. 2).

A second mechanism by which heart and cartilage growth could be impaired is reduced proliferation. BrdU incorporation experiments over the same range of developmental time points showed that proliferation was diminished in the myocardium, endocardium, and branchial tissues of exposed embryos (Fig. 3).

To determine the consequences of reduced proliferation quantitatively, myocardial cell numbers were analyzed using

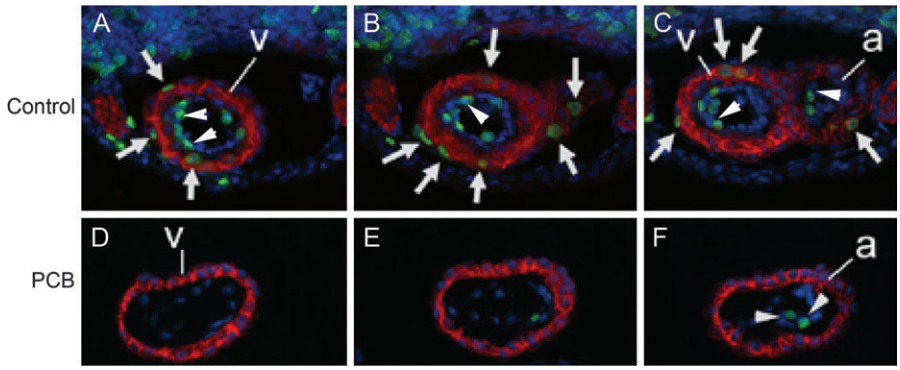

FIG. 3. Myocardial proliferation is impaired. Transverse sections through the hearts of 72 hpf zebrafish. Dorsal is to the top of the image. MF20 (red), myocardium; BrdU (green), proliferating cells; DAPI (blue), nuclei. (A–C) Control (DMSO). (D–F) PCB126 exposed. In each series, the sections are shown close to the atrioventricular border. Abundant proliferation in myocardium (arrows) and endocardium (arrowheads) of controls is almost completely abolished after PCB exposure. a, atrium; v, ventricle.

Tg(*cmlc2*::DsRed2-nuc) fish (Figs. 4A–F). At 48 hpf, there was a small reduction in atrial myocyte numbers in PCB-exposed hearts (Fig. 4G). However, by 72 hpf, atrial myocyte numbers were not significantly different in controls versus exposed fish. In contrast, ventricular myocyte numbers were specifically reduced by approximately 35% in exposed fish at 72 hpf when compared to controls (Fig. 4H). Ventricular cardiomyocytes in the PCB126-exposed embryos also lost volume from 48 hpf, being considerably smaller by 72 and 96 hpf than they had been at 48 hpf and smaller than control cardiomyocytes at the same time points (Figs. 4C and 4F).

To quantify the reduction in size of ventricular cardiomyocytes, we used the Tg(*cmlc2*::DSRed2-nuc) fish double labeled with Zn5, a monoclonal antibody that marks cardiomyocyte cell boundaries. During normal zebrafish cardiogenesis, the heart chambers are established by differential growth and changing morphology of cardiomyocytes in the outer curvature (Auman *et al.*, 2007). In PCB-exposed hearts, these processes were initiated normally as there were no obvious morphological differences between the ventricular myocytes residing at the inner and outer curvatures and clear development of the chambers (Figs. 5A and 5B). However, there were subtle differences in cell size and heart morphology even at this early stage. In many cases, the development of the outer curvature of PCB-exposed hearts appeared restricted to the caudal half of the chamber, making the ventricle appear tear-shaped rather than ellipsoid. Additionally, the myocardial component of the outflow tract and the atrioventricular canal (AVC) appeared less compact in exposed hearts. Calculations of cell size revealed an average reduction of approximately 25%. By 96 hpf, the PCB-exposed ventricular cardiomyocytes were 50% smaller in the outer curvature than in controls (Figs. 5C and 5D). Furthermore, many of these cells had lost much of the boundary marker Zn5 (white arrowheads in Fig. 5D). Cardiomyocytes in the inner curvature did not undergo such dramatic morphological changes.

Outflow Tract Endocardium Is Disrupted

To investigate endothelial/endocardial involvement in the heart phenotype, we used transgenic fish that express GFP in endothelial and endocardial cells. By 48 hpf, outflow tract endocardium appeared to be dysmorphic in 75% of fish investigated (17/24) and was either reduced to a narrow, compact line of endocardial cells, or missing entirely, with no obvious luminal space (Fig. 6B). By 96 hpf, in 100% of cases ($N = 24$), the endocardial lumen of the outflow tract was partially or fully occluded with no sign of outflow valvulogenesis. In 25% of the fish investigated at 96 hpf (5/24), there was complete blockage at the distal limit of the ventricle and no endocardium at all in the outflow tract (Fig. 6E). The myocardial phenotype appeared to be exacerbated in cases where the outflow was blocked completely (Figs. 6D and 6E). Although none of the exposed fish had obvious endocardial occlusion in the AVC, there was no apparent valvulogenesis at 96 hpf, whereas the valve rudiments were apparent in that region in controls (Fig. 6C).

Pifithrin-α Rescues the Heart Phenotype in a p53-Independent Manner

The reduced ventricular proliferation suggested that PCB126 might perturb the cell cycle. Because the cell cycle checkpoint protein p53 is known to block the cell cycle, we adopted a chemical approach and used pifithrin-α, a well-known inhibitor of p53 transcriptional activity (Komarov *et al.*, 1999). Pifithrin-α (1μM) cotreatment with PCB126 restored a normal heart phenotype in over 80% of cases (47/60). Proliferation was restored, pericardial effusion eliminated, and the heart and bulbus arteriosus returned to their usual shape, size, and orientation. Furthermore, Alcian blue staining of the branchial cartilages revealed that jaw development was partially restored (Fig. 7).

In an attempt to duplicate the rescue conferred by chemical suppression of p53, we used p53 morpholino injections at

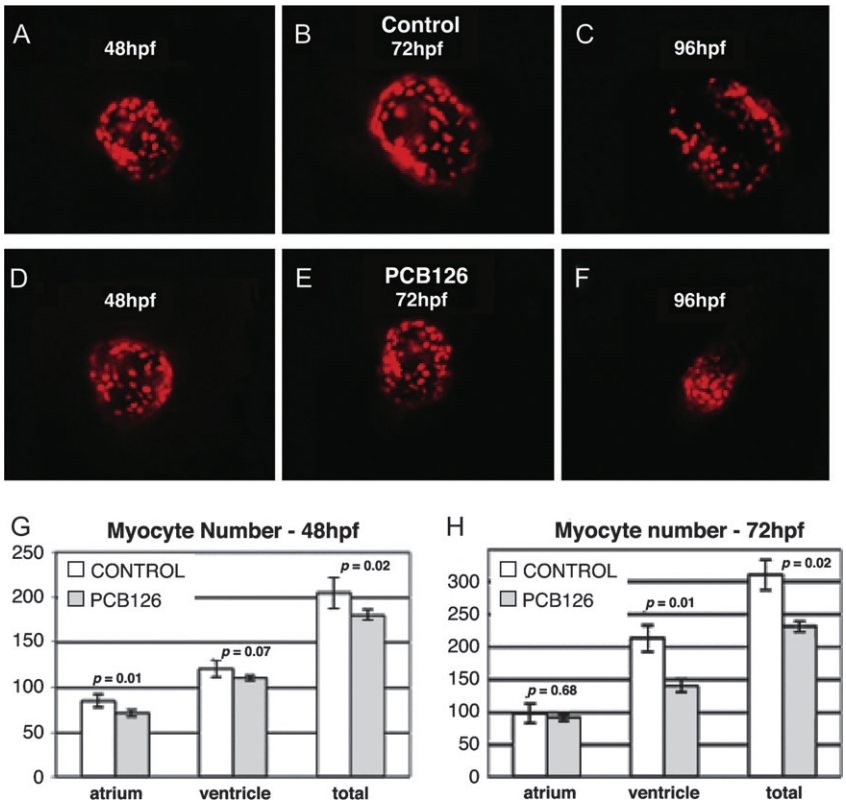

FIG. 4. PCB126 induces a ventricular-specific reduction in the number of myocytes. (A–F) Ventral views of whole-mount Tg(*cmlc2*::DSRed-nuc) transgenic fish, which express red fluorescent protein (RFP) in cardiomyocyte nuclei. Ventricle viewed through the pericardial sac, cranial to the right. (A–C) show normal growth of the ventricle from 48 to 96 hpf in controls. (D–F) show the reduction in size of the PCB-exposed heart over the same time period. The cells of the ventricle become small and clustered (compare panels C and F). Hearts of representative fish were excised, and the cells of the atrium and ventricle were counted. (G) Myocyte counts at 48 hpf. There is a small difference in the number of both atrial and ventricular myocytes at this stage, although the difference in ventricular myocytes is not significant at $p = 0.05$. (H) Myocyte counts at 72 hpf. There is no significant difference in the number of atrial myocytes between control and PCB126-exposed fish, but there is a 35% reduction in the number of ventricular myocytes in the PCB126-exposed fish at this stage ($p = 0.01$). Data were analyzed using two-tailed student's *t*-test. Bars show mean ± SE. $N = 6$ for each group.

several concentrations (Langheinrich *et al*., 2002). No protection against PCB126 was conferred at doses between 4 and 15 ng. However, this morpholino rescued camptothecin-induced apoptosis, showing that p53 had been successfully knocked down (data not shown). As a final test, p53-null mutant fish were exposed to PCB126. These fish were not resistant to the PCB-induced cardiotoxic effect as 100% of the fish developed the heart phenotype ($n = 48$).

Pifithrin-α is a known AHR agonist (Hoagland *et al*., 2005), although the concentration used for rescue in these experiments was well below that calculated to compete with PCB126, which has 10-fold higher binding affinity. To determine whether pifithrin-α acted as a competitive agonist, we used *cyp1a* expression as a measure of AHR activation. Quantitative PCR assays on RNA from whole embryos using primers specific for *cyp1a* showed that pifithrin-α induced a modest increase in message compared to PCB126. The induction of *cyp1a* in fish cotreated with PCB126 and pifithrin-α remained at the level of pifithrin-α treatment alone (Fig. 7G).

The PCB-Induced Heart Phenotype Depends on Cardiac Function

Because endocardial disruption and occlusion of the outflow tract suggested that hemodynamic forces may play a role in the development of the heart phenotype, we eliminated heartbeat and circulation by injection of the cardiac troponin T (*tnnt2*) morpholino (Sehnert *et al*., 2002). Heart function was inhibited in 100% of the *tnnt2* morpholino-injected embryos. Heart development in the morphant embryos was somewhat abnormal in that chamber size appeared slightly larger. Chamber size appeared to be increased in *tnnt2* morphants exposed to PCB126, completely reversing the reduction in chamber size in embryos treated with control morpholinos and exposed to PCB126 (Figs. 7H–K). Interestingly, the PCB-induced jaw phenotype persisted in the morphants, and *cyp1a* was induced in the hearts to a comparable level (44.1- ± 1.4-fold) with the uninjected PCB-treated hearts (61.3- ± 2.0-fold) (Fig. 7L). This suggests that the heart phenotype induced by PCB126 is dependent on cardiac function.

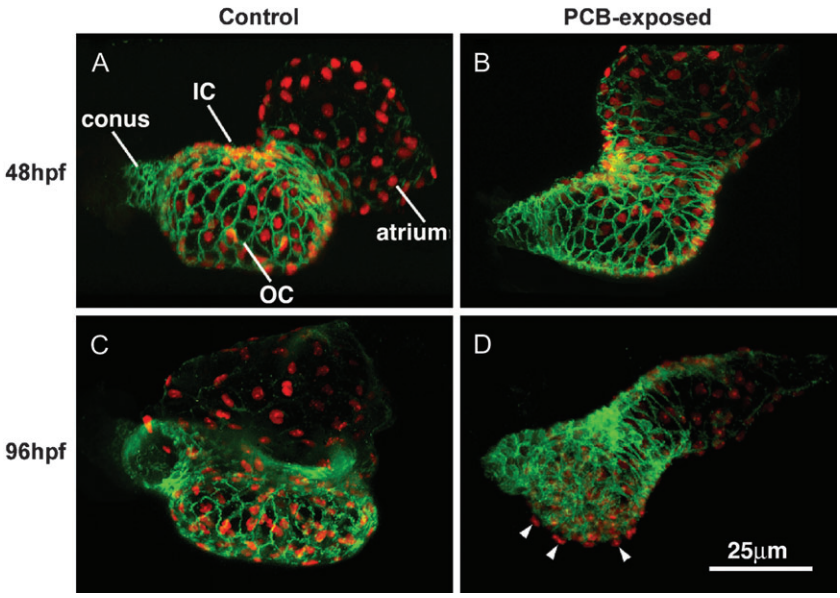

FIG. 5. Ventricular myocytes are reduced in size after PCB exposure. Control (A, C) and PCB exposed (B, D) Tg(*cmlc2*::DsRed-nuc) zebrafish hearts. Nuclei express red fluorescent protein, secondarily detected by anti-DsRed antibody. Myocyte boundaries are labeled with Zn5 antibody (green). Cranial (outflow) to the left of all images. (A, B) Ventral views showing the rightward looping of the heart; (C, D) lateral views. The atrium of the control fish lies dorsal to the ventricle while in the PCB-exposed fish it remains in a more caudal position. White arrowheads in (D) show cardiomyocytes that lack Zn5 boundary marker. Note that Zn5 labeling in the atrium is generally fainter than in the ventricle. However, the perceived stronger labeling in the atrium of PCB-exposed hearts is an artifact of the stretching of the chamber and the signal being amplified by a narrower depth of field in the confocal scanning process (i.e., more scans per cell). IC, inner curvature; OC, outer curvature.

DISCUSSION

Our study presents a comprehensive analysis of the cardiac phenotype induced in zebrafish embryos by exposure to PCB126. The phenotype includes stenotic or obstructed ventricular outflow, underdevelopment of the bulbus arteriosus, disrupted atrioventricular (AV) valve formation, reduction in myocardial cell size, and ventricular myocardial hypoplasia following cell cycle arrest. The similarity of the PCB-induced phenotype to that of HLHS is striking especially in view of the recent linkage of PCBs and dioxins to HLHS in humans (Kuehl and Loffredo, 2006).

Examining possible processes whereby the heart of PCB-exposed fish could diminish in size over time, we established that the phenotype was not caused by cell death. In contrast, proliferation was markedly reduced in PCB-exposed fish, specifically in cardiac and NC-derived branchial tissues. Furthermore, PCB126 induced a ventricular-specific reduction of the number of cardiomyocytes, which became hypoplastic and considerably smaller than in controls by 96 hpf. This is in accord with previous work (Antkiewicz *et al*., 2005), in which TCDD-exposure induced reductions in the total number of zebrafish cardiomyocytes by 48 hpf and a ''ventricular stand-still'' by 5 dpf. In that study, and in this, the atrium of exposed fish continued beating, but the frequency of ventricular contractions began to drop by 72 hpf and was abolished by 5 dpf (data not shown).

The lack of ventricular proliferation in PCB-exposed fish suggested that the cell cycle might be a primary target for perturbation. It has previously been proposed that the AHR may regulate the cell cycle (Elferink, 2003), and microarray data from TCDD-exposed zebrafish hearts suggest that the most reliably affected cluster of genes is involved in cell cycle processes (Carney *et al*., 2006). A direct interaction of the AHR with the retinoblastoma protein (Rb) has been proposed (Ge and Elferink, 1998), and p53 involvement has been suggested to correlate with increased apoptosis (Denison and Nagy, 2003). However, although p53 was implicated in our initial studies where pifithrin-α rescued the PCB-induced heart phenotype, the absence of TUNEL labeling in exposed embryos suggested that cell cycle arrest was not coupled with cell death. Further analysis of *cyp1a* mRNA showed that the phenotypic rescue by pifithrin-α may result from competitive binding of the AHR. It was therefore surprising that cotreatment with PCB126 and pifithrin-α did not cause additive effects but rather maintained levels of message induced by the weaker agonist alone. This highlights the complexity of AHR signaling. Pifithrin-α has also been shown to be a potent CYP1 enzyme inhibitor. The dose of PCB126 and associated level of *cyp1a* induction needed to induce cardiovascular toxicity is not known. Thus, the ability of pifithrin-α to rescue may be related to its ability to block CYP1 enzyme activity, rather than its potential to reduce PCB126 activation of the AHR.

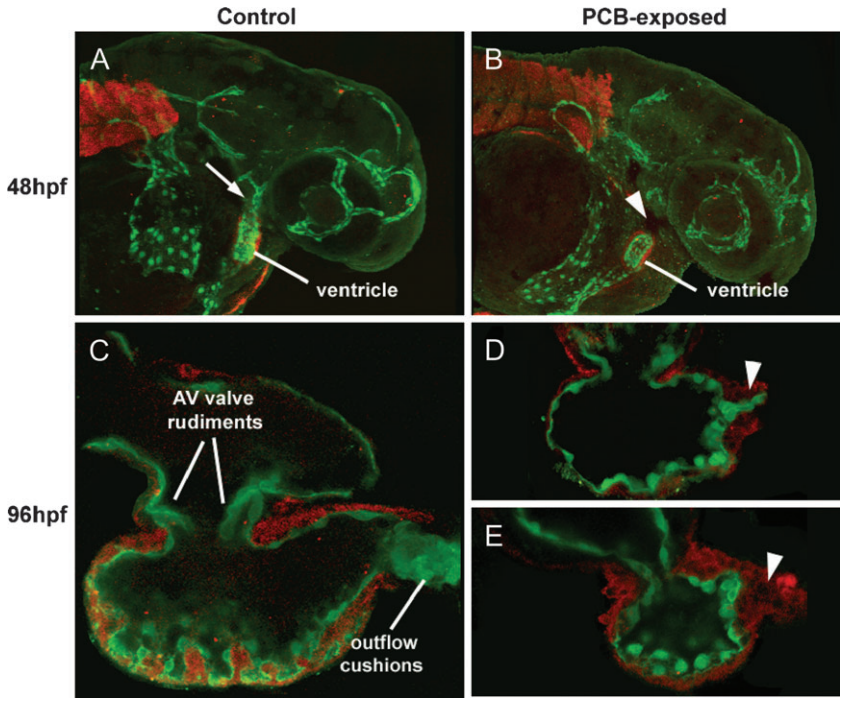

FIG. 6. PCB126 disrupts endocardial development and valvulogenesis. Control and PCB126-exposed Tg(*Flk1*::GFP)^{s843} transgenic zebrafish labeled with MF20 (red). Endothelial/endocardial GFP is secondarily detected with anti-GFP antibody. Cranial to the right, dorsal to the top. (A, B) Composite images generated from confocal z-stacks. (A) At 48 hpf, the endocardium of the control fish is physically continuous with the vascular endothelium (white arrow). (B) Outflow tract endocardium is disrupted in the PCB-exposed fish, and there is no ventricular vascular outlet channel (white arrowhead). (C) 96 hpf control. Confocal sagittal section through the midline of the heart. A continuous endocardium can be seen (green) in close association with the myocardium. AV valve leaflets are well developed, and the outflow cushions show strong GFP expression. (D) PCB-exposed fish with disrupted endocardium in the outflow tract (arrowhead). The lumen is narrow. The AV canal is open, but there is no evidence of valve formation. (E) PCB-exposed fish lacking endocardium in the outflow tract (arrowhead). The ventricle is extremely hypoplastic. The AV canal is open, but narrow.

A plausible mechanism for cell cycle arrest is the failure of myocardial cells to grow to appropriate sizes for the next division. Our data indicate that myocardial cell size is generally smaller than normal, and this is similar to what has been found in human hearts with HLHS (Bohlmeyer *et al.*, 2003). While it is established that cell growth in yeast is coupled to cell cycling through p53 checkpoint arrest, the mechanism for coupling cell size and cell division in metazoans is unknown.

Initial morphological development of the heart was relatively unaffected by PCB126. In the majority of cases, cardiovascular failure became obvious by the appearance of pericardial effusion, blood pooling at the cardiac inflow, and morphological change of the heart. In some extreme cases, mild effusion was seen as early as 24 hpf, indicating that, despite the lack of gross morphological differences, cardiac function may be impaired very early in development. The early, modest reduction in the numbers of atrial myocytes may account for this apparently mild, early-onset phenotype. Regardless, the likelihood of early impaired cardiac function is of particular interest. Any dysmorphology of the heart observed up to 48 hpf is at a developmental stage before addition to the cardiac outflow tract of the bulbus arteriosus, a structure proposed to be akin to the arterial trunk of air-breathing vertebrates (Grimes *et al.*, 2006). By 96 hpf, arterial pole defects included an almost total lack of the bulbus arteriosus and a truncated, stenotic outflow. It seems unlikely that cardiac and arterial trunk dysmorphogenesis would be independent of one another, but the sequence of events suggests that developmental impairment of the bulbus arteriosus (arterial trunk) may be secondary to cardiac dysfunction.

It is possible that PCB126 elicits its cardiotoxic effects by targeting endocardial cells. The AHR and CYP1A are strongly activated in the vascular endothelium of several species (Montie *et al.*, 2008; Omori *et al.*, 2007; Pelclova *et al.*, 2007). Endocardial signaling is a known requirement for myocardial maturation and for the development of trabeculae (Grego-Bessa *et al.*, 2007). Of particular interest is the zebrafish *cloche* mutant, which lacks endocardial cells and in which the ventricular myocardium beats weakly (Stainier *et al.*, 1995).

Utilizing the Tg(*Flk1*::EGFP)^{s843} transgenic zebrafish, we examined the effect of PCB126 on endocardial development. By 96 hpf, PCB126 induced universal disruption of outflow tract endocardium and, in some cases, a complete lack of endocardium within this region, causing occlusion or total blockage of the myocardial component of the outflow (the conus arteriosus—Grimes *et al.*, 2006; Icardo, 2006). It is unclear why outflow endocardium would be specifically targeted by PCB126, but because of the occasional total lack of outflow tract endocardium, one could speculate that this

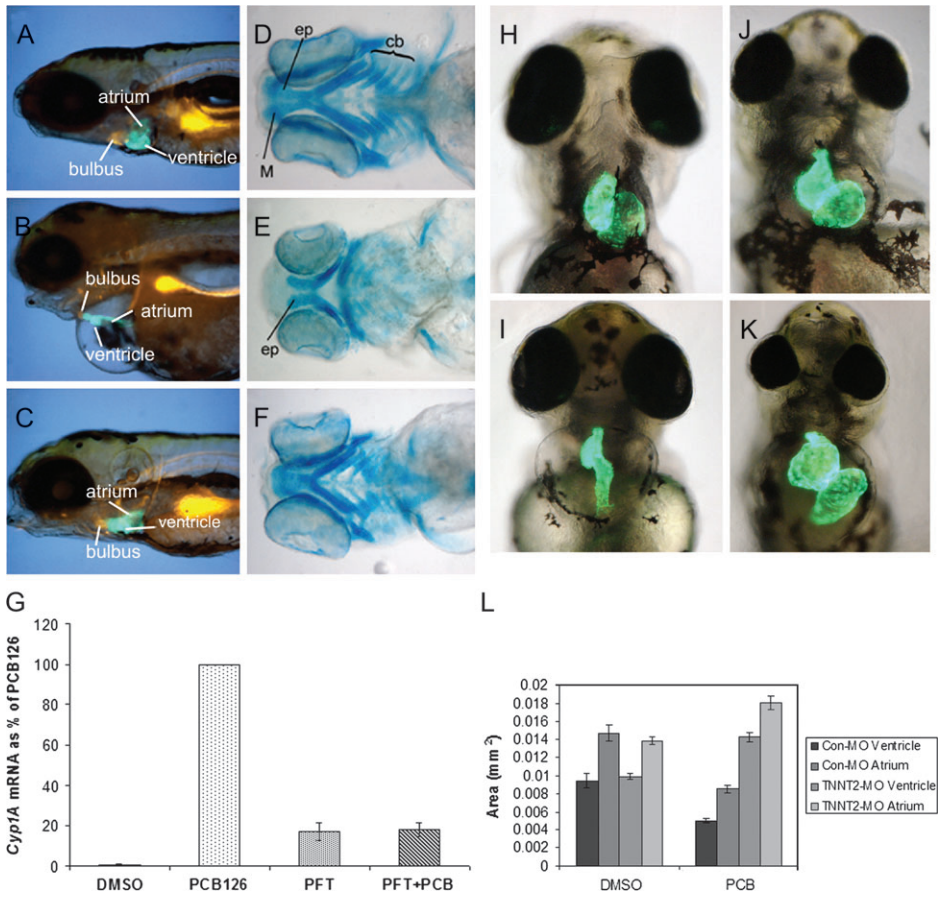

FIG. 7. Two methods of rescuing the PCB126 heart phenotype. (A–C) show 96 hpf wholemount, lateral views of control (A), PCB126-exposed (B) and PCB126/pifithrin-α cotreated (C) Tg(*cmlc2*::GFP) fish, incubated in DAR-4M (red) to label the bulbus arteriosus. Morphology and alignment of the heart structures are restored by pifithrin-α. The jaw phenotype is also rescued by pifithrin-α as seen in lateral views of Alcian blue–stained control (D), PCB126-exposed (E) and PCB126/pifithrin-α cotreated (F) fish. ep, ethmoid plate; M, Meckel's cartilage; cb, ceratobranchials. (G) Quantitative RT-PCR on whole fish lysates showing induction of cyp1a RNA in response to PCB, pifithrin-α, and a combination of the two. Data are represented as % increase of message over controls. Rescue by pifithrin-α appears to be due to competitive inhibition of PCB126 at AHR. (H–K) Ventral views of 72 hpf embryos treated with control morpholino (H, I) or *tnnt2* morpholino (J, K) treated with DMSO (H, J) or PCB126 (I, K). The *tnnt2* morphant hearts appear larger in both DMSO and PCB treatment groups. (L) Area measurements indicating that chamber size is the same or larger in *tnnt2* morphants even when the embryos are exposed to PCB126 (Control-MO/DMSO, $n = 7$; Control-MO/PCB, $n = 11$; *tnnt2*-MO/DMSO, $n = 54$; *tnnt2*-MO/PCB, $n = 57$).

particular cell population has an embryonic origin (spatial or temporal) distinct from ventricular and atrial endocardium. Regardless of this, the data are compelling. Mehta *et al*. (2008) showed that TCDD causes alterations in AV valve development and consequent blood regurgitation in the hearts of zebrafish. This study focused primarily on the development of the AV valve, and it is unclear whether similar outflow occlusion occurs in TCDD-treated embryos.

HLHS has been classified based on the pathologic anatomy of both the aortic and mitral valves (Tchervenkov *et al*., 2006). It has therefore been suggested that valvular and/or endocardial dysfunction may be a primary cause of the condition and that hypoplasia of the ventricle is secondary to the resulting reduced blood flow (Hinton *et al*., 2007). Support for this comes from an experimental embryonic chick model of HLHS in which ligation of the left atrium induces hypoplasia of the left ventricle (Sedmera *et al*., 2002).

To test this hypothesis, we used a morpholino approach to eliminate blood flow. Cardiac troponin T (*tnnt2*) has previously been identified as the gene responsible for the zebrafish silent heart (*sih*) mutation, in which cardiac conduction and contraction are uncoupled so that heart function is not initiated (Sehnert *et al*., 2002). Although the heart of these morphants was slightly dysmorphic, there was no difference between those exposed to PCB126 and controls. Furthermore, the cardiac dysmorphogenesis was consistent with the previously published *sih* phenotype (Sehnert *et al*., 2002). Interestingly, although these experiments strongly suggest a link between cardiac function and hemodynamic forces and the heart phenotype, the jaw phenotype was not rescued in these experiments. This suggests distinct etiologies for the heart and jaw malformations and may account for a lack of reported craniofacial abnormalities in human cases of HLHS.

While it was not possible to determine definitively whether myocardial dysmorphogenesis was secondary to endocardial

disruption and impaired hemodynamics, a model where reduced blood flow through the ventricle leads to secondary hypoplasia is not without precedent (Fishman *et al*., 1978). Recent pedigree analysis suggested that HLHS may be a serious form of valve malformation as there was a high prevalence of valve dysplasia in HLHS subjects and of bicuspid aortic valves in the study subjects' family members, but no familial prevalence of mitral valve dysfunction (Hinton *et al*., 2007). Importantly, outflow valve abnormalities have been described as "universal" in HLHS, whereas mitral valve malformations are only described as "common" (Bharati and Lev, 1984).

It is known that the AHR is highly expressed in many NC-derived tissues including the visceral arches (Abbott and Probst, 1995; Schmidt and Bradfield, 1996). Furthermore, morpholino knockdown of the ARNTs in zebrafish leads to downregulation of transcripts involved in NC development (Wu *et al*., 2006), suggesting that the AHR pathway may be necessary for normal NC development and function. However, expression of *crestin* and *AP2* shows that NC migration is not impaired by PCB126. Furthermore, we found that Alcian blue–stained NC-derived branchial cartilages are all patterned correctly in exposed fish, although they become diminished in size. The failure in growth rather than disrupted patterning is supported by phenotypes arising from a known failure of NC development, such as in the *van gogh* mutant (*tbx1* null) (Piotrowski *et al*., 2003), which reveals a dramatic difference between branchial cartilage patterning defects arising from a failure of NC migration and the PCB-induced phenotype. Two other studies support our conclusion that early NC development is not affected in PCB-treated embryos. Using TCDD, Ivnitski *et al*. (2001) showed increased apoptosis in the developing chick heart. However, they concluded that the apoptotic cells were not of neural crest origin. Another study in zebrafish embryos showed abnormal jaw development caused by TCDD exposure (Teraoka *et al*., 2002). However, because the NC cells have finished forming the lower jaw by 24 hpf and the defective development appeared after that, the investigators concluded that NC migration was unlikely to be a TCDD target.

In summary, although gross signs of cardiotoxicity are very subtle during early stages of development (up to 24 hpf), they suggest that perturbation of cardiogenesis is already occurring. PCB126 toxicity certainly affects both endocardial and myocardial development, specifically in the AVC, ventricle, and arterial pole. A link to hemodynamic forces is strongly suggested by this work. However, the precise nature of this early insult and how it leads to ventricular myocardial cell cycle arrest remains to be elucidated. The zebrafish may be an excellent model in which to investigate these unresolved questions and the etiology of HLHS.

SUPPLEMENTARY DATA

Supplementary Figures 1 and 2 are available online at http://toxsci.oxfordjournals.org/.

FUNDING

National Institutes of Health (R01 70140 to M.L.K.); a Duke Environmental Health Sciences Research Center Pilot Project Grant (to M.L.K and A.C.G.)

ACKNOWLEDGMENTS

The authors thank Ranjula Wijayatunge, Ronald Perez, Kristen Winkler, Trisha Saha, Dr Tim Oliver, Dr David Sedmera, Dr Lisa Satterwhite, Dr Fernando Martinez, and Laura A. Barbosky.

REFERENCES

Abbott, B. D., and Probst, M. R. (1995). Developmental expression of two members of a new class of transcription factors: II. Expression of aryl hydrocarbon receptor nuclear translocator in the C57BL/6N mouse embryo. *Dev. Dyn.* **204,** 144–155.

Antkiewicz, D. S., Burns, C. G., Carney, S. A., Peterson, R. E., and Heideman, W. (2005). Heart malformation is an early response to TCDD in embryonic zebrafish. *Toxicol. Sci.* **84,** 368–377.

Auman, H. J., Coleman, H., riley, H. E., Olale, F., Tsai, H. J., and Yelon, D. (2007). Functional modulation of cardiac form through regionally confined cell shape changes. *PLos Biol.* **5,** e53.

Berghmans, S., Murphey, R. D., Wienholds, E., Neuberg, D., Kutok, J. L., Fletcher, C. D., Morris, J. P., Liu, T. X., Schulte-Merker, S., Kanki, J. P., *et al*. (2005). tp53 mutant zebrafish develop malignant peripheral nerve sheath tumors. *Proc. Natl. Acad. Sci. U.S.A.* **102,** 407–412.

Bharati, S., and Lev, M. (1984). The surgical anatomy of hypoplasia of aortic tract complex. *J. Thoracic Cardiovasc. Surg.* **88,** 97–101.

Bohlmeyer, T. J., Helmke, S., Ge, S., Lynch, J., Brodsky, G., Sederberg, J. H., Robertson, A. D., Minobe, W., Bristow, M. R., and Perryman, M. B. (2003). Hypoplastic left heart syndrome myocytes are differentiated but possess a unique phenotype. *Cardiovasc. Pathol.* **12,** 23–31.

Carney, S. A., Chen, J., Burns, C. G., Xiong, K. M., Peterson, R. E., and Heideman, W. (2006). Aryl hydrocarbon receptor activation produces heart-specific transcriptional and toxic responses in developing zebrafish. *Mol. Pharmacol.* **70,** 549–561.

Carney, S. A., Peterson, R. E., and Heideman, W. (2004). 2,3,7,8-Tetrachlorodibenzo-p-dioxin activation of the aryl hydrocarbon receptor/aryl hydrocarbon receptor nuclear translocator pathway causes developmental toxicity through a CYP1A-independent mechanism in zebrafish. *Mol. Pharmacol.* **66,** 512–521.

Carpenter, A. E., Jones, T. R., Lamprecht, M. R., Clarke, C., Kang, I. H., Friman, O., Guertin, D. A., Chang, J. H., Lindquist, R. A., Moffat, J., *et al*. (2006). CellProfiler: Image analysis software for identifying and quantifying cell phenotypes. *Genome Biol.* **7,** R100.

Cronk, C. E., Pelech, A. N., Malloy, M. E., and McCarver, D. G. (2004). Hypoplastic left heart syndrome in eastern Wisconsin for birth cohorts 1997–1999. *Birth Defects Res.* **70,** 114–120.

Denison, M. S., and Nagy, S. R. (2003). Activation of the aryl hydrocarbon receptor by structurally diverse exogenous and endogenous chemicals. *Annu. Rev. Pharmacol. Toxicol.* **43,** 309–334.

DeWitt, J. C., Millsap, D. S., Yeager, R. L., Heise, S. S., Sparks, D. W., and Henshel, D. S. (2006). External heart deformities in passerine birds exposed to environmental mixtures of polychlorinated biphenyls during development. *Environ. Toxicol. Chem.* **25,** 541–551.

Elferink, C. J. (2003). Aryl hydrocarbon receptor-mediated cell cycle control. *Prog. Cell Cycle Res.* **5,** 261–267.

Ferencz, C., Rubin, J. D., Loffredo, C. A., and Magee, C. M. (1993). In *The Epidemiology of Congenital Heart disease, The Baltimore-Washington Infant Study (1981–1989)*, Vol. 4. Futura Publishing Co., Inc., Mount Kisco, NY.

Fishman, N. H., Hof, R. B., Rudolph, A. M., and Heymann, M. A. (1978). Models of congenital heart disease in fetal lambs. *Circulation* **58,** 354–364.

Fox, K., Zauke, G. P., and Butte, W. (1994). Kinetics of bioconcentration and clearance of 28 polychlorinated biphenyl congeners in zebrafish (Brachydanio rerio). *Ecotoxicol. Environ. Saf.* **28,** 99–109.

Ge, N. L., and Elferink, C. J. (1998). A direct interaction between the aryl hydrocarbon receptor and retinoblastoma protein. Linking dioxin signaling to the cell cycle. *J. Biol. Chem.* **273,** 22708–22713.

Grego-Bessa, J., Luna-Zurita, L., del Monte, G., Bolos, V., Melgar, P., Arandilla, A., Garratt, A. N., Zang, H., Mukouyama, Y. S., Chen, H., *et al.* (2007). Notch signaling is essential for ventricular chamber development. *Dev. Cell.* **12,** 415–429.

Grimes, A. C., Stadt, H. A., Shepherd, I. T., and Kirby, M. L. (2006). Solving an enigma: Arterial pole development in the zebrafish heart. *Dev. Biol.* **290,** 265–276.

Hill, A. J., Bello, S. M., Prasch, A. L., Peterson, R. E., and Heideman, W. (2004). Water permeability and TCDD-induced edema in zebrafish early-life stages. *Toxicol. Sci.* **78,** 78–87.

Hinton, R. B., Jr., Martin, L. J., Tabangin, M. E., Mazwi, M. L., Cripe, L. H., and Benson, D. W. (2007). Hypoplastic left heart syndrome is heritable. *J. Am. Coll. Cardiol.* **50,** 1590–1595.

Hoagland, M. S., Hoagland, E. M., and Swanson, H. I. (2005). The p53 inhibitor pifithrin-alpha is a potent agonist of the aryl hydrocarbon receptor. *J. Pharmacol. Exp. Ther.* **314,** 603–610.

Huang, C. J., Tu, C. T., Hsiao, C. D., Hsieh, F. J., and Tsai, H. J. (2003). Germline transmission of a myocardium-specific GFP transgene reveals critical regulatory elements in the cardiac myosin light chain 2 promoter of zebrafish. *Dev. Dyn.* **228,** 30–40.

Icardo, J. M. (2006). Conus arteriosus of the teleost heart: Dismissed, but not missed. *Anat. Rec. A. Discov. Mol. Cell. Evol. Biol.* **288,** 900–908.

Ivnitski, I., Elmaoued, R., and Walker, M. K. (2001). 2,3,7,8-Tetrachlorodibenzo-p-dioxin (TCDD) inhibition of coronary development is preceded by a decrease in myocyte proliferation and an increase in cardiac apoptosis. *Teratology* **64,** 201–212.

Jin, S. W., Beis, D., Mitchell, T., Chen, J. N., and Stainier, D. Y. (2005). Cellular and molecular analyses of vascular tube and lumen formation in zebrafish. *Development* **132,** 5199–5209.

Jönsson, M. E., Jenny, M. J., Woodin, B. R., Hahn, M. E., and Stegeman, J. J. (2007a). Role of AHR2 in the expression of novel cytochrome P450 1 family genes, cell cycle genes, and morphological defects in developing zebrafish exposed to 3,3′,4,4′,5-pentachlorobiphenyl or 2,3,7,8-tetrachlorodibenzo-p-dioxin. *Toxicol. Sci.* **100,** 180–193.

Jönsson, M. E., Orrego, R., Woodin, B. R., Goldstone, J. V., and Stegeman, J. J. (2007b). Basal and 3,3′,4,4′,5-pentachlorobiphenyl-induced expression of cytochrome P450 1A, 1B and 1C genes in zebrafish. *Toxicol. Appl. Pharmacol.* **221,** 29–41.

Komarov, P. G., Komarova, E. A., Kondratov, R. V., Christov-Tselkov, K., Coon, J. S., Chernov, M. V., and Gudkov, A. V. (1999). A chemical inhibitor of p53 that protects mice from the side effects of cancer therapy. *Science* **285,** 1733–1737.

Kreiling, J. A., Creton, R., and Reinisch, C. (2007). Early embryonic exposure to polychlorinated biphenyls disrupts heat-shock protein 70 cognate expression in zebrafish. *J. Toxicol. Environ. Health A* **70,** 1005–1013.

Kuehl, K. S., and Loffredo, C. A. (2006). A cluster of hypoplastic left heart malformation in Baltimore, Maryland. *Pediatr. Cardiol.* **27,** 25–31.

Langheinrich, U., Hennen, E., Stott, G., and Vacun, G. (2002). Zebrafish as a model organism for the identification and characterization of drugs and genes affecting p53 signaling. *Curr. Biol.* **12,** 2023–2028.

Li, Y. X., Zdanowicz, M., Young, L., Kumiski, D., Leatherbury, L., and Kirby, M. L. (2003). Cardiac neural crest in zebrafish embryos contributes to myocardial cell lineage and early heart function. *Dev. Dyn.* **226,** 540–550.

Luo, R. S., An, M., Arduini, B. L., and Henion, P. D. (2001). Specific pan-neural crest expression of zebrafish crestin throughout embryonic development. *Dev. Dyn.* **220,** 169–174.

Mably, J. D., Mohideen, M. A., Burns, C. G., Chen, J. N., and Fishman, M. C. (2003). Heart of glass regulates the concentric growth of the heart in zebrafish. *Curr. Biol.* **13,** 2138–2147.

Mehta, V., Peterson, R. E., and Heideman, W. (2008). 2,3,7,8-Tetrachlorodibenzo-p-dioxin exposure prevents cardiac valve formation in developing zebrafish. *Toxicol. Sci.* **104,** 303–311.

Montie, E. W., Fair, P. A., Bossart, G. D., Mitchum, G. B., Houde, M., Muir, D. C., Letcher, R. J., McFee, W. E., Starczak, V. R., Stegeman, J. J., *et al.* (2008). Cytochrome P4501A1 expression, polychlorinated biphenyls and hydroxylated metabolites, and adipocyte size of bottlenose dolphins from the Southeast United States. *Aquat. Toxicol.* **86,** 397–412.

Nusslein-Volhard, C., and Dahm, R. (2002). In *Zebrafish. Practical Approach.* Oxford University Press, New York.

Omori, N., Fukata, H., Sato, K., Yamazaki, K., Aida-Yasuoka, K., Takigami, H., Kuriyama, M., Ichinose, M., and Mori, C. (2007). Polychlorinated biphenyls alter the expression of endothelial nitric oxide synthase mRNA in human umbilical vein endothelial cells. *Hum. Exp. Toxicol.* **26,** 811–816.

Orn, S., Andersson, P. L., Förlin, L., Tysklind, M., and Norrgren, L. (1998). The impact on reproduction of an orally administered mixture of selected PCBs in zebrafish (Danio rerio). *Arch. Environ. Contam. Toxicol.* **35,** 52–57.

Pelclova, D., Prazny, M., Skrha, J., Fenclova, Z., Kalousova, M., Urban, P., Navratil, T., Senholdova, Z., and Smerhovsky, Z. (2007). 2,3,7,8-TCDD exposure, endothelial dysfunction and impaired microvascular reactivity. *Hum. Exp. Toxicol.* **26,** 705–713.

Piotrowski, T., Ahn, D. G., Schilling, T. F., Nair, S., Ruvinsky, I., Geisler, R., Rauch, G. J., Haffter, P., Zon, L. I., Zhou, Y., *et al.* (2003). The zebrafish van gogh mutation disrupts tbx1, which is involved in the DiGeorge deletion syndrome in humans. *Development* **130,** 5043–5052.

Robu, M. E., Larson, J. D., Nasevicius, A., Beiraghi, S., Brenner, C., Farber, S. A., and Ekker, S. C. (2007). p53 activation by knockdown technologies. *PLoS Genet.* **3,** e78.

Sato, M., and Yost, H. J. (2003). Cardiac neural crest contributes to cardiomyogenesis in zebrafish. *Dev. Biol.* **257,** 127–139.

Schmidt, J. V., and Bradfield, C. A. (1996). Ah receptor signaling pathways. *Annu. Rev. Cell Dev. Biol.* **12,** 55–89.

Sedmera, D., Hu, N., Weiss, K. M., Keller, B. B., Denslow, S., and Thompson, R. P. (2002). Cellular changes in experimental left heart hypoplasia. *Anat. Rec.* **267,** 137–145.

Sehnert, A. J., Huq, A., Weinstein, B. M., Walker, C., and Fishman, M. (2002). Cardiac troponin T is essential in sarcomere assembly and cardiac contractility. *Nat. Genet.* **31,** 106–110.

Stainier, D. Y. R., Weinstein, B. M., Detrich, H. W., III., Zon, L. I., and Fishman, M. C. (1995). Cloche, an early acting zebrafish gene, is required by both the endothelial and hematopoietic lineages. *Development* **121,** 3141–3150.

Tchervenkov, C. I., Jacobs, J. P., Weinberg, P. M., Aiello, V. D., Beland, M. J., Colan, S. D., Elliott, M. J., Franklin, R. C., Gaynor, J. W., Krogmann, O. N., *et al.* (2006). The nomenclature, definition and classification of hypoplastic left heart syndrome. *Cardiol. Young* **16,** 339–368.

Teraoka, H., Dong, W., Ogawa, S., Tsukiyama, S., Okuhara, Y., Niiyama, M., Ueno, N., Peterson, R. E., and Hiraga, T. (2002). 2,3,7,8-Tetrachlorodibenzo-p-dioxin toxicity in the zebrafish embryo: altered

regional blood flow and impaired lower jaw development. *Toxicol. Sci.* **65,** 192–199.

Thackaberry, E. A., Nunez, B. A., Ivnitski-Steele, I. D., Friggins, M., and Walker, M. K. (2005). Effect of 2,3,7,8-tetrachlorodibenzo-p-dioxin on murine heart development: Alteration in fetal and postnatal cardiac growth, and postnatal cardiac chronotropy. *Toxicol. Sci.* **88,** 2242–2249.

World Health Organization (WHO). (2000). *Polychlorinated Biphenyls (PCBs) in Air Quality Guidelines for Europe*, 2nd ed. World Health Organization Regional Office for Europe; WHO Regional Publications, WHO Press, Geneva, Switzerland, pp. 97–101.

Wu, J. S., Wang, W. D., Ko, C. Y., Chung, H. Y., Chan, Y. C., and Hu, C. H. (2006). *Functions of ARNT2 in zebrafish development. 7th International Meeting on Zebrafish Development and Genetics,* 14–18 June, 2006 Madison, WI.